

SEISMIC EARTH PRESSURES BY STRESS LIMIT ANALYSIS

Panos KLOUKINAS¹, George MYLONAKIS², Costas PAPANTONOPOULOS³ and Dimitrios ATMATZIDIS⁴

ABSTRACT

A closed-form stress plasticity solution is presented for earthquake-induced earth pressures and the distribution of these pressures on gravity retaining walls. The solution is essentially an approximate yield line approach that takes into account the following parameters: (1) weight and friction angle of the soil material, (2) wall inclination, (3) backfill inclination, (4) wall roughness, (5) surcharge at soil surface, and (6) horizontal and vertical seismic acceleration. Both active and passive conditions are considered by means of different inclinations of stress characteristics in the backfill. Results are presented in the form of dimensionless graphs and charts that elucidate the salient features of the problem. Comparisons with established numerical solutions for gravity loading, such as those of Chen and Sokolovskii show satisfactory agreement (maximum error for active pressures about 10%). While the solution does not faithfully satisfy equilibrium everywhere in the medium (and hence cannot be classified as rigorous lower bound), extensive comparisons with numerical results indicate that it consistently over- and under-predicts active and passive pressures, respectively. Hence the solution can be viewed as an approximate lower bound, rather than a mere predictor of limit thrusts. In the second part of the paper, the solution is extended to determine the distribution of limit pressures on a gravity wall. To achieve this, variable soil strength with depth is considered to simulate soil arching in the backfill based on the kinematics of the wall. Compared to Coulomb and Mononobe-Okabe equations, the proposed solution is algebraically simpler and safer, as typically overestimates active pressures and underestimates the passive. In addition, it provides a rational means for determining the distribution of limit thrusts on the back of the wall.

Keywords: retaining structures, soil-structure interaction, limit analysis, Mononobe-Okabe, Coulomb

INTRODUCTION

The classical equations of Coulomb (Coulomb, 1776) and Mononobe-Okabe (Okabe, 1926; Mononobe & Matsuo, 1929) are being widely used for determining earth pressures due to gravitational and earthquake loads, respectively. It is well known, that both solutions fall into the family of *kinematic* solutions of limit analysis. These solutions are based on kinematically admissible failure mechanisms in conjunction with a yield criterion and a flow rule for the soil material, both of which are enforced along a pre-specified failure surface (Chen, 1975). Stresses outside the failure surface are not examined and, thereby, equilibrium in the medium is generally not satisfied. In the realm of associative and convex materials, solutions of this type are inherently *unsafe* that is, they underestimate active pressures and overestimate the passive.

A second group of limit-analysis methods, the *stress* solutions, make use of stress fields that satisfy the equilibrium equations and the stress boundary conditions, without violating the failure criterion

¹ Graduate Student, Department of Civil Engineering, University of Patras, Greece, Email: pkloukin@upatras.gr

² Professor, Department of Civil Engineering, University of Patras, Greece, Email: mylo@upatras.gr

³ Professor, Department of Civil Engineering, University of Patras, Greece, Email: cip@upatras.gr

⁴ Professor, Department of Civil Engineering, University of Patras, Greece, Email: dka@upatras.gr

anywhere in the medium (Atkinson, 1981; Davis & Selvadurai, 2002). On the other hand, the kinematics of the response is not examined and, therefore, compatibility of deformations in the medium is generally not satisfied. For convex materials, formulations of this type are inherently *safe* that is, they overestimate active pressures and underestimate the passive. The best known such solution is that of Rankine, the applicability of which is limited by the assumptions of horizontal backfill, vertical wall and smooth soil-wall interface. Owing to difficulties in deriving pertinent stress fields for all but the simplest geometries, the vast majority of limit-analysis solutions in geotechnical design are of the kinematic type (Chen, 1975; Kramer 1996; Richards & Elms 1979). To the best of the authors' knowledge, no closed-form solution of the stress type is available for estimating seismic earth pressures.

Notwithstanding the theoretical significance and practical appeal of the Coulomb and Mononobe-Okabe solutions, these formulations can be criticized on the following important aspects: (1) in the context of limit analysis, their predictions are unsafe; (2) their accuracy (and safety) diminishes in the case of passive pressures on rough walls, (3) the mathematical expressions are complicated and difficult to verify, (4) the distribution of contact stresses on the wall are not predicted (typically assumed proportional with height following Rankine's solution), (5) optimization of the failure mechanism is required in the presence of multiple loads, to determine a stationary (optimum) value of soil thrust, and (6) stress boundary conditions are not satisfied, as the yield surface does not generally emerge at the soil surface at the expected angles of $45^\circ \pm \phi/2$.

In light of the above arguments, it appears that the development of a closed-form solution of the stress type for assessing seismically-induced earth pressures would be desirable. It will be shown that the proposed solution is mathematically simpler than the existing kinematic solutions, offers satisfactory accuracy (maximum error for active pressures less than 10%), yields results typically on the safe side, satisfies stress boundary conditions and predicts the point of application of soil thrust. Apart from its intrinsic theoretical interest, the proposed analysis can be used for the assessment and improvement of other related methods.

PROBLEM DEFINITION AND MODEL DEVELOPMENT

The problem under investigation is depicted in Figure 1: a slope of dry cohesionless soil retained by an inclined gravity wall, is subjected to plane deformations (plane strain) under the combined action of gravity (g) and seismic body forces ($a_h * g$) and ($a_v * g$) in the horizontal and vertical direction, respectively. The problem parameters are: the height (H) and inclination (ω) of the wall, the inclination (β) of the slope; the roughness (δ) of the wall-soil interface; the friction angle (ϕ) and unit weight (γ) of the soil material, and the surface surcharge (q). Since backfills typically consist of granular materials, cohesion in the soil and the soil-wall interface are not considered. Note that the retained soil is considered rigid* before yielding, so the seismic force is uniform within the backfill.

We can see from Figure.1 that the resultant body force is acting at an angle ψ_e from vertical

$$\tan \psi_e = \frac{a_h}{1 - a_v} \quad (1)$$

* This hypothesis is not essential from a limit analysis viewpoint. It is merely a convenient assumption regarding the nature of earthquake action in the backfill.

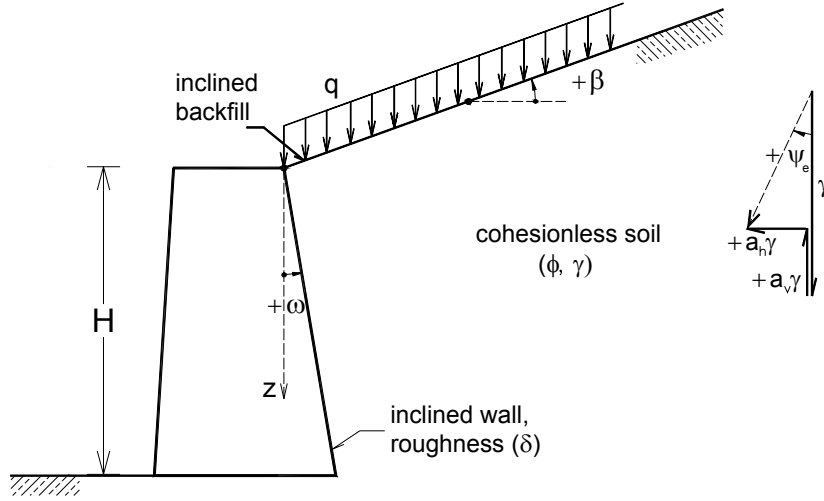


Figure 1. The problem under consideration

Positive acceleration a_h (i.e., $\psi_e > 0$) denotes inertial action towards the wall, which maximizes active thrust. Conversely, negative a_h (i.e., $\psi_e < 0$) denotes inertial action towards the backfill, which minimizes passive resistance. To prevent slope failure under active conditions, the seismic angle ψ_e should not exceed the difference between the friction angle and the slope inclination. Therefore, the following constraint applies (Ebeling et al, 1992):

$$\psi_e < \phi - \beta \quad (2)$$

To analyze the problem, the backfill is divided into two main zones subjected to different stress fields, as shown in Figure 2: the first zone (zone A) is located close to the soil surface, whereas the second (zone B) close to the wall. In both zones the soil is assumed to be in a condition of impending yielding under the combined action of gravitational and seismic forces. The same assumption is adopted for the soil-wall interface, which, however, is subjected exclusively to contact stresses. A transition zone between zones A and B is introduced later on.

Fundamental to the proposed analysis is the assumption that stresses close to the soil surface can be well approximated by those in an *infinite slope*, as shown in Figure 2. In zone A, the inclined soil element shown in hatch is subjected to canceling actions along its vertical sides. Thus equilibrium is achieved solely under body forces and contact stress acting at its bottom face. Based on this physically motivated hypothesis, stresses σ_β and τ_β at the base of the inclined element are determined from the well-known expressions:

$$\sigma_\beta = \left(\gamma z + \frac{q}{\cos \beta} \right) \cos^2 \beta \quad (3a)$$

$$\tau_\beta = \left(\gamma z + \frac{q}{\cos \beta} \right) \sin \beta \cos \beta \quad (3b)$$

which are valid for static conditions ($a_h = a_v = 0$) and satisfy the stress boundary conditions at the surface. Equations (3) suggest that the ratio of shear to normal stresses is constant ($\tan \beta$) at all depths, and that points at the same depth are subjected to equal stresses. Note that due to static determinacy and anti-symmetry, the above relations are independent of material properties and are asymptotically *exact* at large distances from the wall.

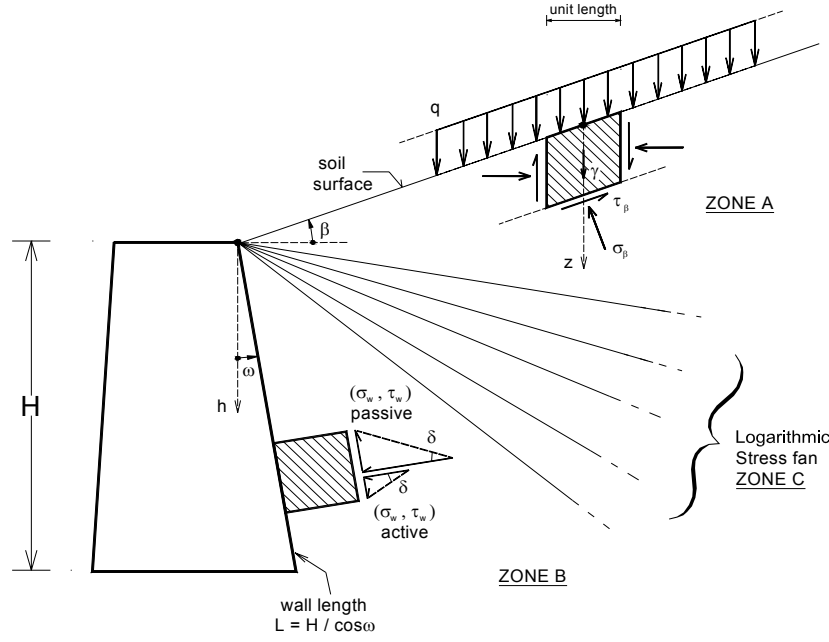


Figure 2. Stress fields close to soil surface (A), wall (B), and transition zone (C)

Considering the material to be in a condition of impending yielding, the Mohr circle of stresses in zone A is depicted in Figure 3a. The different locations of the stress point $(\sigma_\beta, \tau_\beta)$ for active and passive conditions and the different inclinations of the major principal plane (indicated by heavy lines) are apparent in the graph. For points in zone B, it is assumed that stresses are functions exclusively of the vertical coordinate and obey the strength criterion at the frictional soil-wall interface, as shown in Figure 2. Accordingly, at orientations inclined at an angle ω from vertical,

$$\tau_w = \sigma_w \tan \delta \quad (4)$$

where σ_w and τ_w denote the normal and shear tractions on the wall, at depth z . The above equation is asymptotically *exact* for points in the vicinity of the wall. The corresponding Mohr circle of stresses is depicted in Figure 3b. The different signs of shear tractions for active and passive conditions follow the directions shown in Figure 2 (i.e., passive wall tractions pointing upward, active tractions pointing downward), which comply with the kinematics of the problem. This is in contrast with the widespread view that stress solutions totally ignore the displacement field (Papantonopoulos & Ladanyi, 1973).

Based on the foregoing, it becomes evident that the orientation of principal planes (and thereby stress characteristics) in the two zones is different and varies for active and passive conditions. In addition, the mean stresses S_A and S_B (Figure 3) generally do not coincide, which suggests that a Rankine type solution based on a continuous stress field in the backfill is not possible. To determine the separation of mean stresses S_A and S_B and ensure a smooth transition in the orientation of principal planes in the two zones, a logarithmic *stress fan* is adopted, centered at the top of the wall (Figure 2). In the interior of the fan, principal stresses are gradually rotated by the angle θ separating the major principal planes in the two zones, as shown in Figure 4. This additional condition is written as (Chen, 1975):

$$S_B = S_A \exp(\mp 2\theta \tan \phi) \quad (5)$$

The negative sign in the above equation pertains to the active case ($S_B < S_A$) and vice versa. Equation (5) is an exact solution of the governing Kötter equations for a weightless material and, thereby, it is accurate for a weightless fan and approximate for a fan with weight (Davis & Selvadurai, 2002).

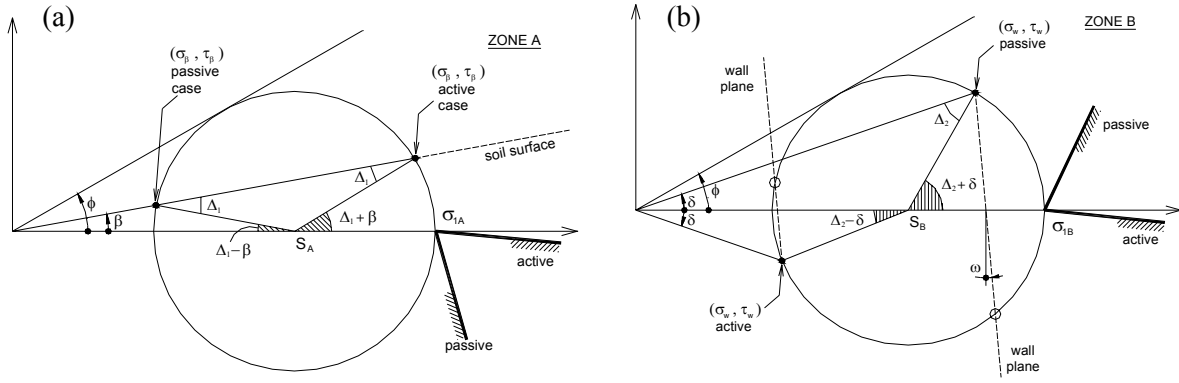


Figure 3. Mohr circles of stresses and inclination of major principal planes in zones A and B.

Solution without Earthquake Loading

The total thrust on the wall due to surcharge and gravity is obtained by the well-known expression:

$$P = K_q q H + \frac{1}{2} K_\gamma \gamma H^2 \quad (6)$$

which is reminiscent (though not equivalent) of the bearing capacity equation of a strip surface footing on cohesionless soil. In the above equation, K_q and K_γ denote the earth pressure coefficients due to surcharge and self-weight, respectively. From Figures 3 and 4, integrating the contact tractions over the height of the wall, it is a matter of straightforward algebraic manipulations to show that the earth pressure coefficient K_γ is given by

$$K_\gamma = \frac{\cos(\omega - \beta) \cos \beta}{\cos \delta \cos^2 \omega} \left[\frac{1 \mp \sin \phi \cos(\Delta_2 \mp \delta)}{1 \pm \sin \phi \cos(\Delta_1 \pm \beta)} \right] \exp(\mp 2\theta \tan \phi) \quad (7)$$

and

$$2\theta = \Delta_2 \mp (\Delta_1 + \delta) + \beta - 2\omega \quad (8)$$

where Δ_1 and Δ_2 denote the Caquot angles (Caquot & Kerisel, 1948; Sokolovskii, 1965) given by

$$\sin \Delta_1 = \frac{\sin \beta}{\sin \phi}, \quad \sin \Delta_2 = \frac{\sin \delta}{\sin \phi} \quad (9, 10)$$

The convention regarding double signs in the above equations is as before. Note that the upper signs suffice for describing both active and passive conditions, if negative values for ϕ and δ are assumed in the passive case. This is discussed in a later section of the article. It is also straightforward to show that the surcharge coefficient K_q is related to K_γ through the simple expression

$$K_q = K_\gamma \frac{\cos \omega}{\cos(\omega - \beta)} \quad (11)$$

which coincides with the kinematic solution of Chen & Liu (1990) obtained using a Coulomb mechanism. Note that for a horizontal backfill ($\beta = 0$), coefficients K_q and K_γ coincide regardless of wall inclination. Equation (11) represents an *exact* solution for a weightless material with surcharge.

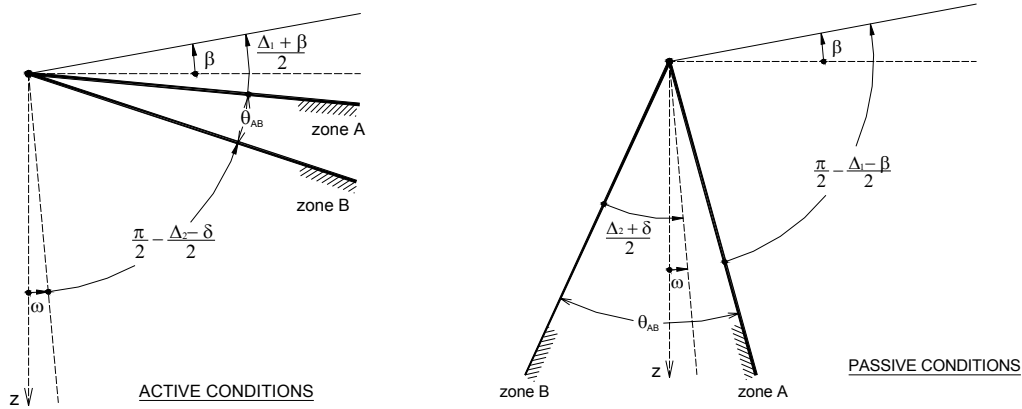


Figure 4. Rotation of major principal planes between zones A and B for active and passive conditions.

Solution including Earthquake Loading

Recognizing that earthquake action imposes a resultant thrust in the backfill inclined at a constant angle ψ_e from vertical (Figure 1), it becomes apparent that the seismic problem does not differ fundamentally from the static problem, as the former can be obtained from the latter through a rotation of the reference axes by the angle ψ_e , as shown in Figure 5. In other words, considering ψ_e does not add an extra physical parameter to the problem, but simply alters the values of the other variables.

This property of *similarity* was apparently first employed by Briske (1927) and later by Terzaghi (1943) and Arango (Seed & Whitman, 1970; Ebeling et al, 1992) for the analysis of related problems. Application of the concept to the present problem yields the following algebraic transformations, according to the notation of Figure 5:

$$\beta^* = \beta + \psi_e, \quad \omega^* = \omega + \psi_e \quad (12a, b)$$

$$H^* = H \cos(\omega + \psi_e) / \cos \omega, \quad (13)$$

$$q^* = q(1 - a_v) / \cos \psi_e, \quad \gamma^* = \gamma(1 - a_v) / \cos \psi_e \quad (14a, b)$$

The modification in the values of γ and q is due to the change in length of the corresponding vectors (Figure 1), as a result of seismic action. To obtain Eqn (14b) it has been tacitly assumed that the surcharge responds to the earthquake motion in the same manner as the backfill. Note that this is not an essential hypothesis - just a convenient (reasonable) assumption from an analysis viewpoint. Understandably, the strength parameters ϕ and δ are invariant to the transformation. In the light of the above, the soil thrust including earthquake action can be determined from the modified expression:

$$P_E = K_q^* q^* H^* + \frac{1}{2} K_\gamma^* \gamma^* H^{*2} \quad (15)$$

in which parameters β , ω , H , γ , and q have been replaced by their transformed counterparts. The symbols K_q^* and K_γ^* denote the surcharge and self-weight coefficients in the modified geometry, respectively. Substituting Eqns (12) - (14) in Eqn (15) yields the modified earth pressure coefficient

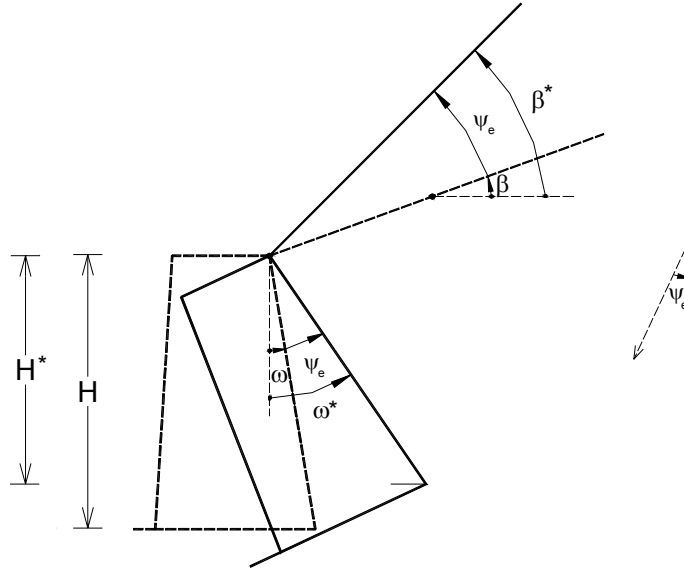


Figure 5. Similarity transformation based on a rotation of the reference axes for analyzing the seismic case as a gravitational problem. Note that the rotation should be performed in the opposite (clockwise) direction for the passive case.

$$K_{\gamma E} = \frac{\cos(\omega - \beta) \cos(\beta + \psi_e)}{\cos \psi_e \cos \delta \cos^2 \omega} \left[\frac{1 \mp \sin \phi \cos(\Delta_2 \mp \delta)}{1 \pm \sin \phi \cos[\Delta_1^* \pm (\beta + \psi_e)]} \right] \exp(\mp 2\theta_E \tan \phi) \quad (16)$$

which encompasses seismic action and can be used in the context of Eqn (6) [with γ being multiplied by $(1-a_v)$]. In the above equation,

$$2\theta_E = \Delta_2 \mp (\Delta_1^* + \delta) + \beta - 2\omega - \psi_e \quad (17)$$

is twice the revolution angle of principal stresses in the two zones under seismic conditions, following Eqns (9) and (12a). The seismic earth pressure coefficient K_{qE} is obtained from Eqn (11), as in the gravitational problem, with K_γ being replaced by $K_{\gamma E}$.

Evidently, the above equations are simpler than those of Coulomb and Mononobe-Okabe and possess a solid physical basis. In addition, they can be derived essentially by inspection, without requiring optimization of equilibrium/energy equations. This is particularly important for cases involving combinations of loads such as gravity and surcharge. Note that, since equilibrium is not rigorously satisfied within the stress fan, the proposed solution should not be viewed as a *rigorous* bound. It will be used in this work as an approximate bound, or merely as predictor of earth pressures. Nevertheless, extensive comparisons against rigorous numerical results presented in the following section, indicate that the solution yields safe predictions for both active and passive pressures. This is evident from the comparisons of the numerical data – despite the fact that an exact solution to the problem does not exist.

Distribution and point of application of soil thrust

As mentioned earlier, the widely used kinematic-type solutions (Coulomb, Mononobe–Okabe), do not provide information on the distribution of stresses on the back of the wall, but simply adopt the hydrostatic distribution as a sufficient approximation for design. The same limitation applies to more rigorous computer-based kinematic solutions (e.g., Chen & Liu 1990).

On the other hand, in classical stress solutions (Rankine 1857, Terzaghi 1943), the hydrostatic distribution stems naturally from the formulation. This is due to the linear variation of stresses with depth in the Rankine zone close to the soil surface (Eqn 3a), which is not altered within the stress fan and close to the wall. Since in the realm of pseudo-dynamic analyses no essential difference between static and seismic excitation exists, the distribution of earth pressures is assumed linear with depth.

It is experimentally known, however, that this distribution is not hydrostatic. Two major mechanisms are responsible for this deviation - both relating to the basic assumptions on the material behavior and the kinematics of the problem. First, soil mass responds dynamically and, thereby, the distribution of accelerations (i.e., body forces) is not uniform with depth. This effect is incorporated in available elastodynamic solutions (e.g., Veletsos & Younan 1994, Langousis et al. 2006). Secondly, the distribution of earth pressures changes for different kinematic constraints of the wall (e.g., rotation about base or top), which relate directly to arching in the backfill. The redistribution of stresses due to arching leads to changes in the magnitude and point of application of soil thrust.

Following Dubrova (Harr 1966, Chen & Liu 1990), it is assumed that soil strength is mobilized gradually with height in the backfill for rotational modes of the wall. Accordingly, for the estimation of soil thrusts, the strength parameters (friction angle ϕ , wall roughness δ) are considered variable with depth. Contrary to the classical Dubrova method, the proposed solution determines directly tractions on the wall in the form:

$$\sigma_w(h) = \gamma h \frac{\cos(\omega - \beta) \cos \beta}{\cos^2 \omega} \left[\frac{1 - \sin \phi(h) \cos(\Delta_2(h) - \delta(h))}{1 + \sin \phi(h) \cos(\Delta_1(h) + \beta)} \right] \exp[-2 \theta_{AB}(h) \tan \phi(h)] \quad (18)$$

and

$$\tau_w(h) = \sigma_w(h) \tan \delta(h) \quad (19)$$

in which the constant values ϕ and δ have been replaced by functions of depth. Equations (18) and (19) yield passive pressures for negative values of ϕ and δ . Functions $\phi(h)$ and $\delta(h)$ are used to describe the transition of stresses from geostatic (K_0) conditions to failure, where ϕ attains its higher values. In this context, $\phi(h)$ and $\delta(h)$ do not describe stress capacity, but merely stress *mobilization* with depth. Following Dubrova, these functions can be assumed, as a first approximation, linear or bi-linear. In the present study, the trapezoidal forms $\phi(h)$ shown in Figure 6 are adopted. Function $\delta(h)$ is assumed of the same form as $\phi(h)$, based on the proportionality relation (Harr 1966):

$$\delta(h) = m\phi(h), \quad 0 < m < 1 \quad (20)$$

Model Verification and Results

Presented in Table 1 are numerical results for gravitational active and passive pressures (K_{Ay} , K_{Py}) from the present solution and established solutions from the literature. The predictions are in good agreement (largest discrepancy about 10%), with the exception of Coulomb's method which significantly over-predicts passive pressures. Moving from the top to the bottom of each column, an increase in K_{Ay} values and a decrease in K_{Py} values can be observed. This is easily understood given the non-conservative nature of the first two solutions (Coulomb, Chen), and the conservative nature of the last two (Sokolovskii, proposed).

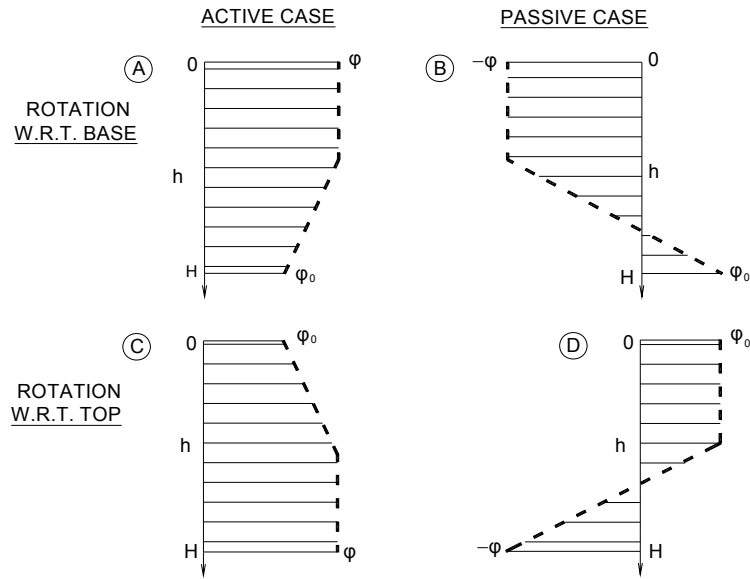


Figure 6. Variation of effective friction angle ϕ for various kinematic conditions of the wall.

Table I: Comparison of results for active and passive earth pressures predicted by various methods ; $\beta = 0^\circ$ (modified from Chen & Liu, 1990)

| a. K_{Ay} – values | | | | | | | | | | |
|--|------------|------------|------------|------------|------------|------------|------------|------------|-------------|------------|
| ω | 0° | | | | | | 20° | | -20° | |
| ϕ | 20° | | 30° | | 40° | | 30° | | 30° | |
| δ | 0° | 10° | 0° | 15° | 0° | 20° | 0° | 15° | 0° | 15° |
| Coulomb | 0.490 | 0.447 | 0.333 | 0.301 | 0.217 | 0.199 | 0.498 | 0.476 | 0.212 | 0.180 |
| Kinematic Limit Analysis (Chen & Liu 1990) | 0.490 | 0.448 | 0.333 | 0.303 | 0.217 | 0.200 | 0.498 | 0.476 | 0.218 | 0.189 |
| Slip line (Sokolovskii 1965) | 0.490 | 0.450 | 0.330 | 0.300 | 0.220 | 0.200 | 0.521 | 0.487 | 0.229 | 0.206 |
| Proposed Stress Limit Analysis | 0.490 | 0.451 | 0.333 | 0.305 | 0.217 | 0.201 | 0.531 | 0.485 | 0.237 | 0.217 |
| b. K_{Py} – values | | | | | | | | | | |
| Coulomb | 2.04 | 2.64 | 3.00 | 4.98 | 4.60 | 11.77 | 2.27 | 3.162 | 5.34 | 12.91 |
| Kinematic Limit Analysis (Chen & Liu 1990) | 2.04 | 2.58 | 3.00 | 4.70 | 4.60 | 10.07 | 2.27 | 3.160 | 5.09 | 8.92 |
| Slip line (Sokolovskii 1965) | 2.04 | 2.55 | 3.00 | 4.62 | 4.60 | 9.69 | 2.16 | 3.16 | 5.06 | 8.45 |
| Proposed Stress Limit Analysis | 2.04 | 2.52 | 3.00 | 4.44 | 4.60 | 8.92 | 2.13 | 3.157 | 4.78 | 7.07 |

Results for gravitational active pressures on a rough inclined wall obtained according to three different methods as a function of the slope angle β , are shown in Figure 7a. The performance of the proposed solution is good (maximum deviation from Chen's solution about 10% - despite the high friction angle of 45°) and elucidates the conservative nature of the predictions compared to an upper bound analysis. The performance of the simplified solution of Caquot and Kerisel (1948) versus that of Chen & Liu (1990) is as expected. Corresponding predictions for passive pressures are given in Figure 7b, for a wall with negative backfill slope inclination, as a function of the wall roughness δ . The agreement of

the various solutions, given the sensitivity of passive pressure analyses is very satisfactory. Of particular interest are the predictions of Sokolovskii's (1965) and Lee & Herington's (1972) methods, which, surprisingly, exceed those of Chen for rough walls. This trend is particularly pronounced for horizontal backfill and δ above about 10° , as discussed by Chen & Liu (1990).

Results for active seismic pressures as a function of the friction angle ϕ , are shown in Figure 8a for the common case of a rough vertical wall with horizontal backfill. The predictions of the proposed analysis are conservative in all cases and in good agreement with the results from the M-O and the kinematic limit analysis of Chen & Liu [1990] (maximum deviation 3%). The corresponding graph for the passive condition is presented in Figure 8b. The predictions of the stress solutions are, understandably, lower than those of Chen and Liu, whereas M-O predictions are very high (i.e., unconservative) – especially for friction angles above approximately 37 degrees. Given the sensitivity of passive pressure analyses, the performance of the proposed method is very satisfactory.

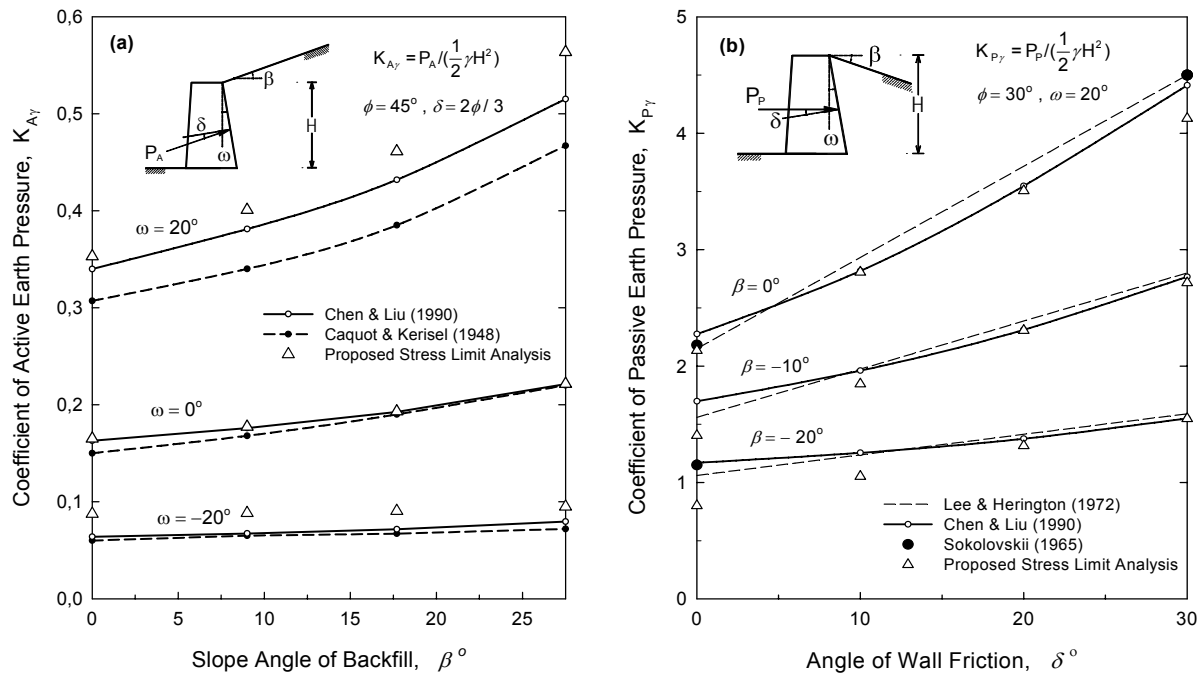


Figure 7. Comparison of results for active and passive earth pressures predicted by different methods. (modified from Chen 1975; Chen & Liu 1990)

A set of results for active seismic pressures are shown in Figure 9, for a reference friction angle of 40° . The following interesting observations can be made: *First*, the predictions of the proposed analysis are in good agreement with the results from the kinematic analysis of Chen & Liu (1990), over a wide range of material and geometric parameters. *Second*, the present analysis is conservative in all cases. *Third*, close to the slope stability limit (Figure 9b), or for high accelerations and large wall inclinations (Figure 9a), Chen's predictions are less accurate than those of the elementary M-O solution. In the same extreme conditions, the proposed solution becomes exceedingly conservative, exceeding M-O predictions by about 35%. Note that whereas the M-O and the proposed solution brake down in the slope stability limit, Chen's solution allows (spurious) mathematical predictions of active thrust beyond instability, as evident in Figure 9b. *Fourth*, with the exception of the aforementioned extreme cases, Chen's and M-O predictions remain close over the whole range of parameters examined. The improvement in the predictions of the former over the latter is marginal.

Figures 10 and 11 present stress distributions based on the present solution (Eqn 18), compared with published experimental results and finite-element simulations. The predictions of the proposed model are comparable to both numerical and experimental results.

Finally Figure 12 depicts the elevation of stress resultant predicted from the proposed method for different kinematic conditions. Interestingly, the point of application of active thrust on a wall rotating around the base is located below $H/3$, contrary to the recommendations by Seed & Whitman (1970). The change in elevation of total thrust with increasing seismic coefficient a_h is marginal.

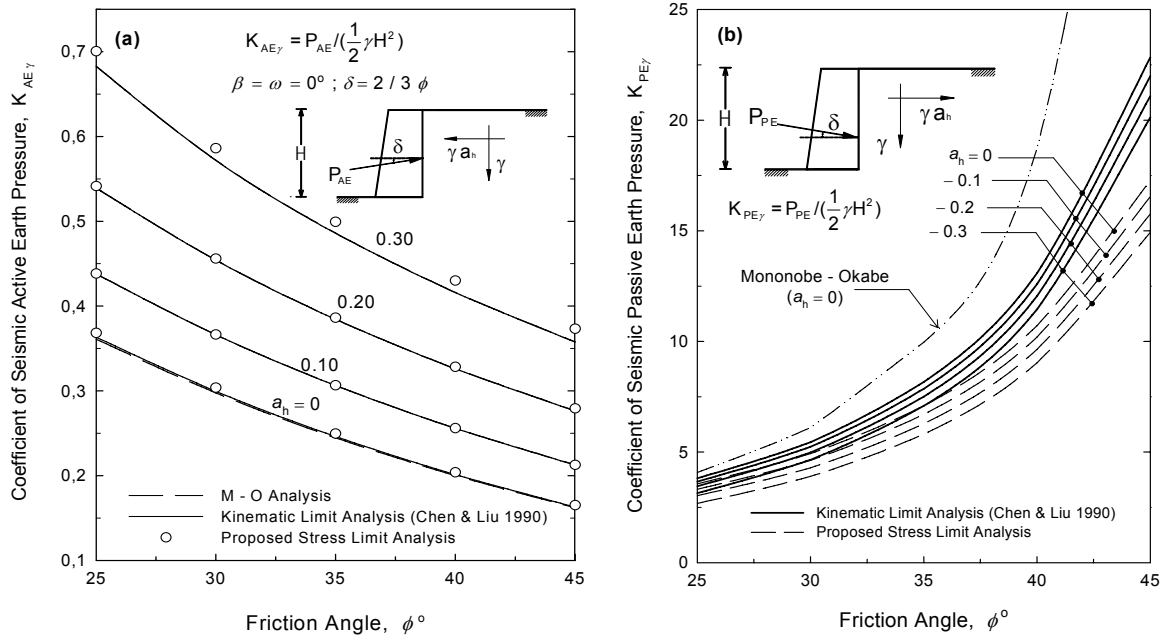


Figure 8. Comparison of results for active and passive seismic resistance on a rough wall, predicted by different methods. (modified from Chen & Liu 1990)

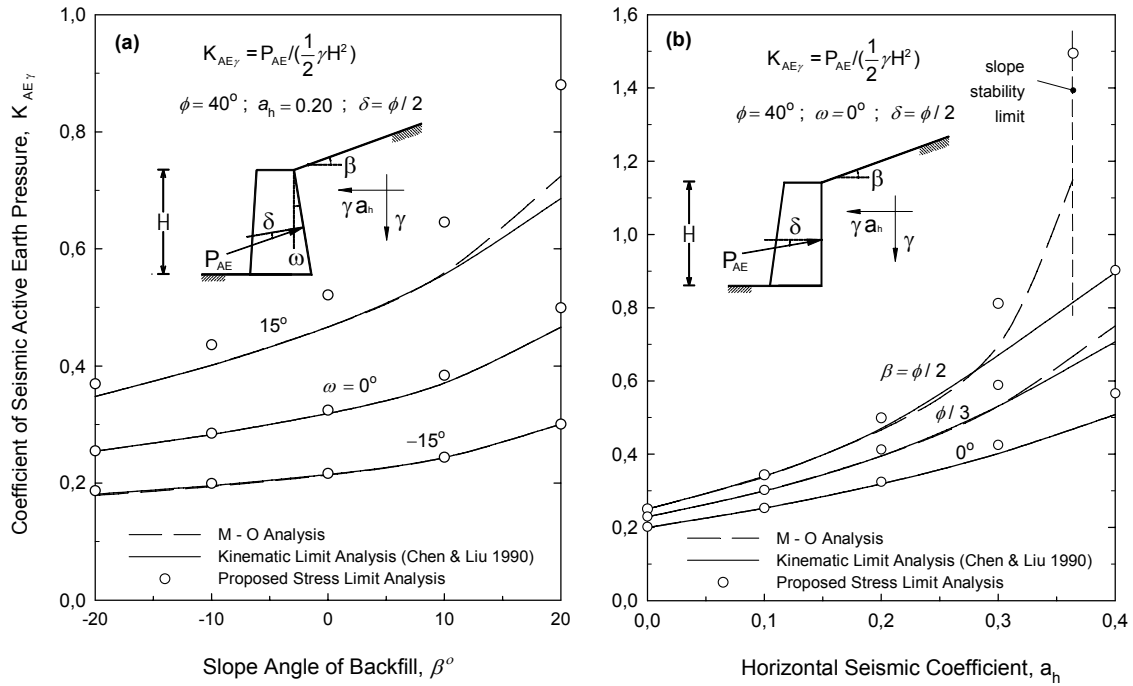


Figure 9. Comparison of results for active seismic pressures on a rough wall with various geometric parameters, predicted by different methods. (modified from Chen & Liu 1990)

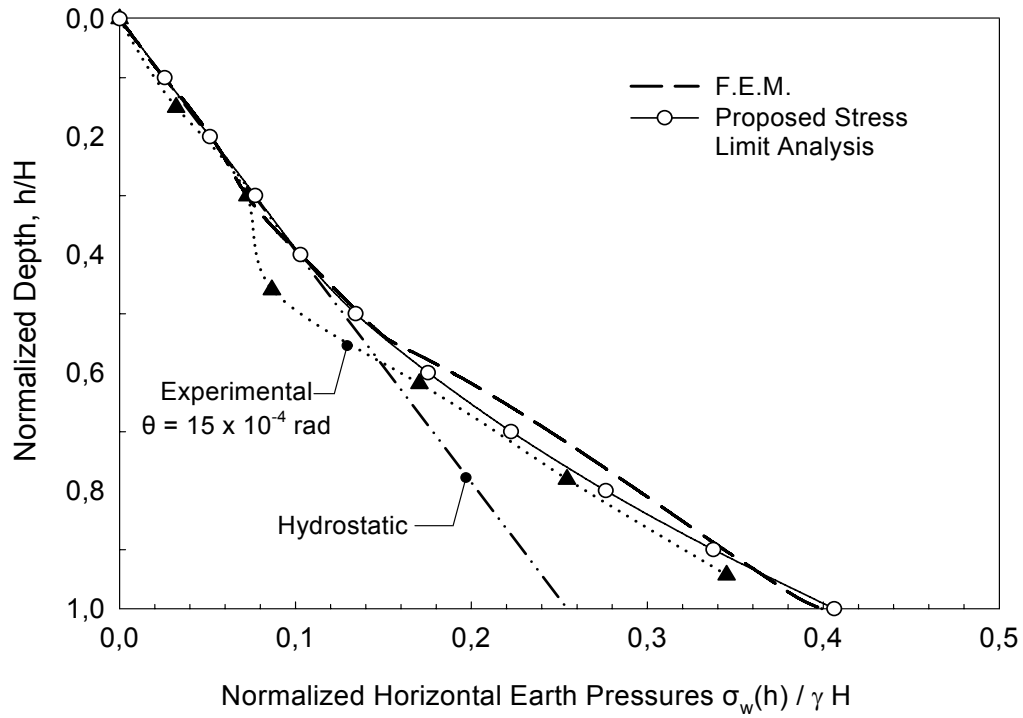


Figure 10. Comparison with experimental results for active rotation about the wall base (modified from Fang & Ishibashi 1986; $\gamma = 15.3 \text{ kN/m}^3$, $H = 1.02 \text{ m}$, $\phi = 33.4^\circ$ and $\delta = 16.7^\circ$)

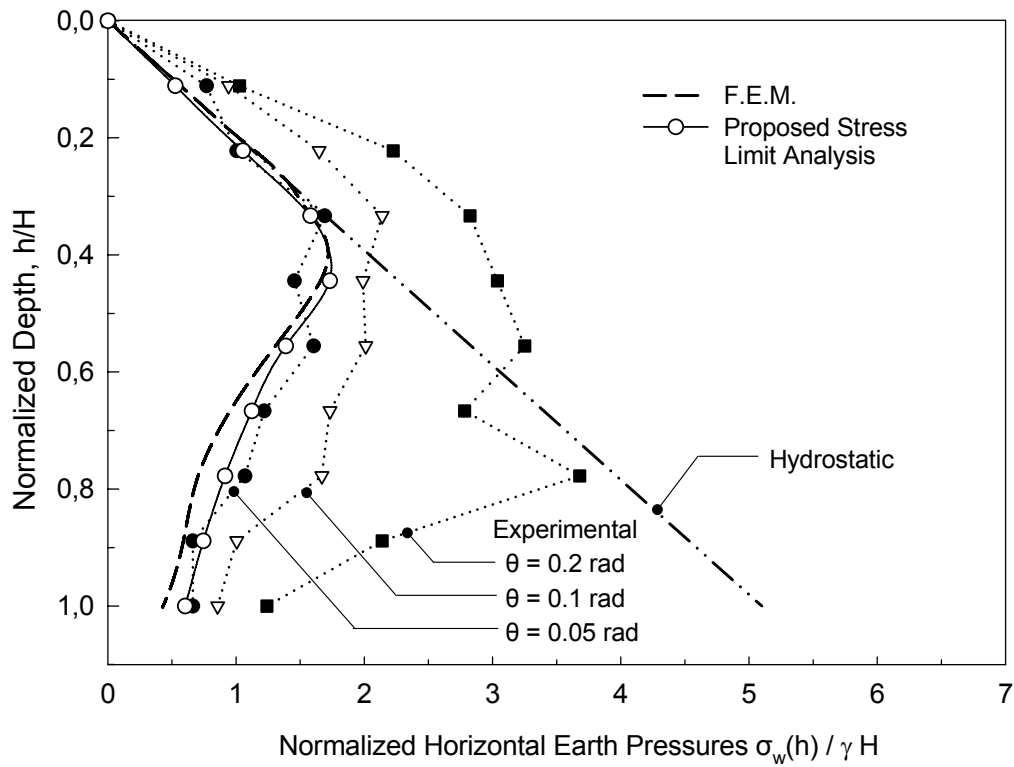


Figure 11. Comparison with experimental results for passive rotation about the wall base (modified from Fang et. al. 1994; $\gamma = 15.5 \text{ kN/m}^3$, $H = 0.45 \text{ m}$, $\phi = 30.9^\circ$ and $\delta = 19.2^\circ$)

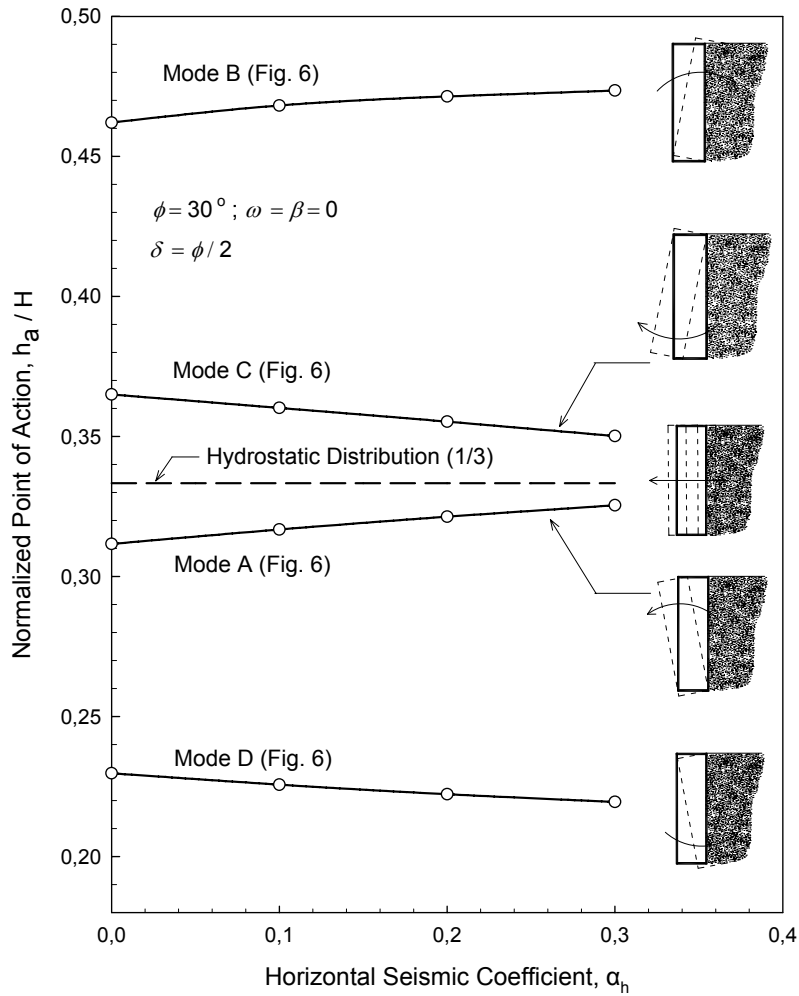


Figure 12. Point of application of total thrust for different kinematic conditions

CONCLUSIONS

A stress plasticity solution was presented for determining gravitational and earthquake-induced earth pressures on gravity walls retaining cohesionless soil. The proposed solution incorporates idealized, yet realistic wall geometries and material properties. The following are the main conclusions of the study:

- (1) The proposed solution is mathematically simpler than the Coulomb and Mononobe-Okabe equations.
- (2) Extensive comparisons with established numerical solutions indicate that the proposed solution is safe, as it over-predicts active pressures and under-predicts passive resistances. This property appears to hold, despite the lack of an exact solution to be used as reference.
- (3) For active pressures, the accuracy of the solution is excellent (maximum observed deviation from numerical data about 10%). The largest deviations occur for high seismic accelerations, high friction angles, steep backfills, and large negative wall inclinations.
- (4) For passive resistance, the predictions are also satisfactory. However, the error is larger - especially at high friction angles. Nevertheless, the improvement over the M-O predictions is dramatic.
- (5) The seismic problem can be deduced from the corresponding gravitational problem through a revolution of the reference axes by the seismic angle ψ_e (Figure 5). This similarity suggests that Coulomb and M-O solutions are essentially equivalent.

(6) Stress limit analysis is particularly suitable for determining traction distributions on the wall. Adopting suitable distributions for ϕ and δ with depth, active and passive conditions (and all intermediate stages) can be described by a single equation (Eqn 18), which is not possible with the Coulomb and M-O solutions. Functions $\phi(h)$ and $\delta(h)$ must be different in active and passive conditions – a requirement not recognized in the classical work of Dubrova. Comparisons against experimental measurements and finite-element solutions showed satisfactory agreement.

REFERENCES

- Atkinson, J. (1981), Foundations and slopes, *McGraw Hill*, London.
- Briske, R. (1927), "Die Erdbebensicherheit von Bauwerken", *Die Bautechnik*, Vol 5, 425- 430.
- Caquot, A. and Kerisel, L. (1948), Traité de mécanique des sols, *Gauthier-Villars*, Paris.
- Chen, W.F. (1975), Limit analysis and soil plasticity, *Developments in geotechnical engineering*, Elsevier, Amsterdam.
- Chen, W.F., Liu, X.L. (1990), Limit analysis in soil mechanics, *Elsevier*, Amsterdam.
- Coulomb, C.A. (1776), "Essai sur une application des regles de maximis et minimis a quelques problemes de stratique relatifs a l' architecture". *Memoires de Mathematique et de Physique. Presentes a l' Academie Royale des Sciences*; Paris, 7, 343-382.
- Davis, R.O. and Selvadurai, A.P.S. (2002), Plasticity and Geomechanics, *Cambridge University Press*, Cambridge.
- Dubrova G.A. (1963). *Interaction of Soil and Structures*. Rehnoy Transport, Moscow, U.S.S.R.
- Ebeling, R.M., Morrison, E.E., Whitman, R.V., Liam Finn, W.D. (1992), A Manual for Seismic Design of Waterfront Retaining Strutures, *US Army Corps of Engineers*, Tech. Report ITL-92-11.
- Fang Y.S. and Ishibashi I. (1986). "Static earth pressures with various wall movements". *Journal of Geotechnical Engineering*, ASCE 112, No 3, pp. 317 – 333.
- Fang Y.S., Chen T.J., and Wu B.F. (1994). "Passive earth pressures with various wall movements". *Journal of Geotechnical Engineering*, ASCE 120, No 8, pp. 1307 – 1323.
- Harr M. (1966). *Foundation of Theoretical Soil Mechanics*, McGraw – Hill, New York, NY.
- Kramer, S.L., (1996), Geotechnical Earthquake Engineering, *Prentice Hal*.
- Kloukinas, P., (2006), "Gravitational and Seismic Earth Pressures by Stress Limit Analysis", Ms Thesis, University of Patras, Greece (in Greek with extended English summary).
- Lee, I.K. and Herington, J.R. (1972), "A theoretical study of the pressures acting on a rigid wall by a sloping earth or rock fill", *Geotechnique*, 22, No 1, 1-26.
- Mononobe, N., Matsuo, O. (1929), On the determination of earth pressure during earthquakes, *Proceeding of the World Engineering Congress*, Tokyo, vol 9, 179-187.
- Okabe, S. (1924), "General theory on earth pressure and seismic stability of retaining walls and dams", *Journal of the Japanese Society of Civil Engineers*, 10, 6, 1277-1323.
- Papantonopoulos, C. and Ladanyi, B. (1973), "Analyse de la Stabilité des Talus Rocheux par une Methode Generalisee de l'Equilibre Limite", *Proceedings, 9th Canadian Rock Mechanics Symposium*, Montreal, 167-196 (in French).
- Psarropoulos P., Klonaris G., and Gazetas G., "Seismic Response of Retaining Walls". Proc., 4th Hellenic Conference on Geotechnical and Geoenvironmental Engineering, Vol. 2, 377-385, 2001.
- Richards, R. and Elms, D.G. (1979), Seismic behavior of gravity retaining walls,. *Journal of the Geotechnical Engineering Division*, ASCE. 105, 449-64
- Seed HB, Whitman, R.V. (1970), Design of earth retaining structures for dynamic loads, *Proceedings of specialty conference on lateral stresses in the ground and design of earth retaining structures*, ASCE, Ithaca, New York, 103-147.
- Sokolovskii, V.V. (1965), Statics of granular media, *Pergamon Press*, New York.
- Terzaghi, K., (1943), Theoretical soil mechanics, *John Wiley & Sons Inc.*, New York.
- Veletsos A.S. and Younan A.H. (1994). "Dynamic soil pressures on rigid retaining walls", *Earthquake Engineering and Structural Dynamics*, 23, pp. 275 – 301.
- Whitman, R.V. and Liao, S. (1985), Seismic Design of Gravity Retaining Walls, *US Army Corps of Engineers*, Miscellaneous paper GL-85-1